Excitations of ^1P levels of zinc by electron impact on the ground state

Dmitry V. Fursa,[1,*] Igor Bray,[1] R. Panajotović,[2] D. Šević,[2] V. Pejčev,[2] D. M. Filipović,[2,3] and B. P. Marinković[2]
[1]*Centre for Atomic, Molecular and Surface Physics, Murdoch University, Perth 6150, Australia*
[2]*Institute of Physics, Belgrade, P.O. Box 68, 11080 Belgrade, Serbia and Montenegro*
[3]*Faculty of Physics, University of Belgrade, 11001 Belgrade, Serbia and Montenegro*
(Received 7 March 2005; published 11 July 2005)

We present results of a joint theoretical and experimental investigation of electron scattering from the $4s^2\ ^1S$ ground state of zinc. The $4s4p\ ^1P^o$ and $4s5p\ ^1P^o$ differential cross sections were measured at scattering angles between 10° and 150° and electron-energies of 15, 20, 25, 40, and 60 eV. Corresponding convergent close-coupling calculations have been performed and are compared with experiment.

DOI: 10.1103/PhysRevA.72.012706 PACS number(s): 34.80.Dp

I. INTRODUCTION

Electron scattering from zinc has been the subject of renewed interest over the last few years due the possibility of using zinc as a replacement for mercury in high-pressure discharge lamps [1] and the associated requirement for accurate collision data. The aim of our joint experimental and theoretical research program is to provide a data set of reliable *e*-Zn collision data. We start with an investigation of the strongest and consequently the most important excitation processes involving excitation of the $^1P^o$ states from the ground state.

There are only a few reported experimental studies for excitation of the $^1P^o$ states of zinc. The $4\,^1P^o$ excitation function has been measured recently by Shpenik *et al.* [2] from threshold to 15 eV and was found to be in good agreement with earlier measurements of the optical excitation function by the same group [3]. Williams and Bozinis [4] presented differential cross sections (DCS's) at a single incident electron energy of 40 eV. More recently the DCS's for ^1S-$^1P^o$ excitations at small scattering angles were reported by Panajotović *et al.* [5] and found to be in rather poor agreement with the earlier measurements [4].

Theoretical results for $^1P^o$ excitations are even more scarce. Kaur *et al.* [6] have applied the relativistic distorted-wave approximation (RDWA) to calculate $4\ ^1P^o$ DCS at 10, 20, and 40 eV. These calculations proved to be in poor agreement with the latest DCS measurements [5]. A detailed study of low-energy elastic scattering and excitations has been conducted recently by Zatsarinny and Bartschat [7] using an *R*-matrix method, presenting the energy dependence of the angle-integrated cross sections. Comparison of the *R*-matrix results with the $4\ ^1P^o$ measurements of Shpenik *et al.* [2] indicated a significant discrepancy.

The purpose of this paper is to present a joint experimental and theoretical study of $^1P^o$ excitations in zinc with the aim of addressing the present disagreement between theory and experiment. We report on extending the earlier low-angle measurements of Panajotović *et al.* [5] to intermediate and large scattering angles which allows for a significantly more stringent test of the theoretical methods. Additionally, convergent close-coupling (CCC) calculations of *e*-Zn scattering were conducted and compared with experimental data. The CCC calculations will also independently verify the low-energy *R*-matrix results of Zatsarinny and Bartschat [7] and extend theoretical predictions to larger incident electron energies.

The paper is organized as follows. In Sec. II we present details of the experimental method, and in Sec. III the CCC calculations are described. Section IV presents the discussion of the results, and in Sec. V we formulate the conclusions and indicate future directions. Atomic units are used throughout the paper unless specified otherwise.

II. EXPERIMENTAL METHOD

The apparatus is the same as the one used to determine *e*-Zn small-angle DCS's [5]. It consists of a conventional crossed-beam electron spectrometer with the basic design described by Chutjian [8]. Briefly, hemispherical energy selectors in both the monochromator and analyzer are made of molybdenum, while all cylindrical lenses are made of gold-plated OFHC copper. The "zoom" lens is placed at the exit of monochromator in order to provide constant focus in the energy range from 10 to 100 eV. The residual magnetic field in the interaction region was less than 0.1 μT achieved by double μ-metal shielding. The primary electron current was in the range from 10 to 50 nA. The analyzer could be rotated from −30° to +150° with respect to the primary electron beam.

The energy scale was calibrated by measuring the position of the resonance feature in the elastic scattering attributed to the threshold energy for the excitation of the $4\ ^3P$ state of Zn at 4.03 eV. In order to observe this resonance structure, it was necessary to achieve the energy resolution of 40 meV. The uncertainty in the energy scale was 300 meV. The position of the zero-scattering angle was determined before each angular distribution measurement by checking the symmetry of the scattered electron signal at positive and negative angles with respect to the unscattered electron beam. The uncertainty in angular scale was 0.5° while overall angular resolution of the present experimental setup was 1.5°.

*Electronic address: d.fursa@murdoch.edu.au

TABLE I. Ionization energies (eV) of negative-energy states (relative to the Zn^+ ground state) in the CCC calculations. The experimental data are from Moore [24]. States are labeled by the major configuration.

Label	CCC	Experiment	Label	CCC	Experiment
$4s^2\ ^1S$	9.394	9.394	$4s4f\ ^3F$	0.855	0.859
$4s4p\ ^3P$	5.342	5.340	$4s4f\ ^1F$	0.855	0.860
$4s4p\ ^1P$	3.541	3.598	$4s7s\ ^3S$	0.639	0.746
$4s5s\ ^3S$	2.748	2.739	$4s6d\ ^1D$	0.562	0.585
$4s5s\ ^1S$	2.436	2.477	$4s7s\ ^1S$	0.561	0.715
$4s5p\ ^3P$	1.792	1.793	$4s5f\ ^3F$	0.543	0.549
$4s4d\ ^1D$	1.628	1.650	$4s5f\ ^1F$	0.543	0.549
$4s4d\ ^3D$	1.595	1.611	$4s6d\ ^3D$	0.540	0.565
$4s5p\ ^1P$	1.568	1.594	$4s7p\ ^3P$	0.444	0.593
$4s6s\ ^3S$	1.282	1.281	$4s7p\ ^1P$	0.365	0.564
$4s6s\ ^1S$	1.186	1.206	$4s6f\ ^3F$	0.300	0.381
$4s6p\ ^3P$	0.945	0.952	$4s6f\ ^1F$	0.300	
$4s5d\ ^1D$	0.910	0.921	$4s7d\ ^1D$	0.242	0.406
$4s5d\ ^3D$	0.884	0.891	$4s7d\ ^3D$	0.205	0.389
$4s6p\ ^1P$	0.864	0.888			

TABLE III. Experimental differential cross sections and errors given in parentheses (in units of 10^{-22} m^2/sr) for electron impact excitations of the $4s5p\ ^1P^o$ level from the ground state of zinc.

Angle (deg)	20 eV	25 eV	40 eV
10	48.2 (2.0)	73.2 (3.8)	107 (12)
15	25.5 (9.7)	36.3 (1.3)	41.8 (3.4)
20	15.1 (0.2)	18.7 (0.400)	12.0 (0.4)
30	4.18 (0.12)	3.85 (0.15)	1.60 (0.13)
40	1.38 (0.067)	1.19 (0.082)	0.357 (0.058)
50	0.708 (0.051)	0.506 (0.053)	0.103 (0.033)
60	0.376 (0.036)	0.229 (0.037)	0.0406 (0.0215)
65			0.0316 (0.0183)
70	0.159 (0.024)	0.142 (0.030)	0.0329 (0.0209)
80	0.0842 (0.0166)	0.0987 (0.0238)	0.0582 (0.0283)
90	0.0455 (0.0131)	0.0674 (0.0158)	0.0316 (0.0200)
100	0.0231 (0.0090)	0.0533 (0.0189)	0.0249 (0.0172)
110	0.0267 (0.0079)	0.0709 (0.0216)	0.0189 (0.0150)
120	0.0466 (0.0139)	0.0982 (0.0260)	0.0121 (0.0117)
125			0.00822 (0.00743)
130	0.0774 (0.0171)	0.129 (0.027)	0.00778 (0.00704)
135			0.0115 (0.0109)
140	0.113 (0.021)	0.173 (0.034)	0.0158 (0.0149)
150	0.149 (0.024)	0.245 (0.041)	0.0232 (0.0176)

To produce a metal-vapor beam from ultrapure zinc granules, we used a resistively heated oven made of titanium. The oven nozzle aspect ratio was 0.075. Monitoring of temperature at the bottom and at the top of the crucible was necessary to provide stable conditions for the target beam. Higher temperature at the top end protected the nozzle from clogging, while constant temperature at the bottom (670 K) provided the effusive atomic flow. The corresponding metal-vapor pressure was approximately 10 Pa while the background pressure was kept below 5 mPa.

TABLE II. Experimental differential cross sections and errors (in units of 10^{-22} m^2/sr) given in parentheses for electron impact excitations of the $4s4p\ ^1P^o$ level from the ground state of zinc.

Angle (deg)	15 eV	20 eV	25 eV	40 eV	60 eV
10	1040 (140)	1520 (240)	1660 (210)	1370 (180)	669 (87)
15	536 (75)	614 (95)	574 (73)	320 (42)	
20	264 (36)	252 (39)	192 (25)	64.4 (9.5)	31.6 (4.2)
25	138 (19)		71.3 (9.2)	20.2 (5.6)	
30	75.9 (9.9)	50.6 (8.2)	34.3 (4.5)	9.21 (1.23)	
40	24.2 (1.7)	15.9 (2.1)	10.0 (1.3)	2.49 (0.35)	2.08 (0.41)
50	11.1 (1.1)	6.17 (0.65)	3.17 (0.42)	0.599 (0.095)	
60	5.84 (0.69)	2.33 (0.32)	1.03 (0.17)	0.395 (0.073)	1.26 (0.326)
70	2.87 (0.36)	0.858 (0.106)	0.493 (0.106)	0.442 (0.084)	
80	1.25 (0.16)	0.316 (0.051)	0.336 (0.114)	0.376 (0.073)	0.518 (0.211)
90	0.476 (0.079)	0.193 (0.046)	0.268 (0.117)	0.241 (0.049)	
100	0.199 (0.042)	0.240 (0.051)	0.222 (0.125)	0.122 (0.030)	0.260 (0.150)
105	0.178 (0.042)				
108			0.189 (0.134)	0.0963 (0.0218)	
110	0.246 (0.055)	0.343 (0.072)	0.197 (0.139)	0.100 (0.030)	
120	0.400 (0.064)	0.466 (0.071)	0.250 (0.151)	0.0966 (0.0277)	0.168 (0.119)
130	0.661 (0.091)	0.755 (0.105)	0.578 (0.156)	0.0717 (0.0249)	
140	0.971 (0.112)	1.30 (0.120)	0.979 (0.196)	0.133 (0.037)	0.240 (0.139)
150	1.30 (0.13)	2.18 (0.25)	1.46 (0.18)	0.349 (0.070)	0.155 (0.110)

TABLE IV. Experimental integrated cross sections and errors given in parentheses (in units of 10^{-20} m^2) for electron impact excitations of the $4s4p\,^1P^o$ and $4s5p\,^1P^o$ states from the ground state of zinc.

Energy (eV)	$4s4p\,^1P^o$	$4s5p\,^1P^o$
15	4.29 (1.07)	
20	5.50 (1.38)	0.220 (0.059)
25	5.87 (1.47)	0.300 (0.081)
40	5.70 (1.43)	0.367 (0.099)
60	4.77 (1.19)	

III. CALCULATION METHOD

Zinc can be accurately modeled as an atom with two active valence electrons above an inert $[\mathrm{Ar}]3d^{10}$ core. The CCC method for electron scattering from quasi-two-electron atoms has been detailed by Fursa and Bray [9], and its applications to alkali-earth atoms (Be, Mg, Ca, Sr, Ba) and Hg have been presented in Refs. [10–14]. Here we give only details specific to e-Zn scattering and present some recent modifications to the CCC method.

Zinc wave functions have been obtained using the same procedure as applied to other quasi-two-electron atoms [9]. Specifically, we used a large set of Laguerre functions for $l \leqslant 3$ to diagonalize the one-electron Zn^+ Hamiltonian. The number of orbitals, $N(l)$, and exponential falloffs $\alpha(l)$ are (27,2.3), (28,2.1), (27,1.7), and (23,1.4). A phenomenological one-electron polarization potential with Zn^{2+} core static dipole polarizability $\alpha_c=2.6$ [15] and cutoff radius $r_c=1.53$ has been added to Zn^+ Hamiltonian in order to model core excitation processes. We retain only nine lowest s and p orbitals, eight lowest d orbitals, and five lowest f orbitals starting from the valence $n=4$ shell. The above one-electron orbitals are used to construct a set of all allowed two-electron antisymmetric configurations of the form $4snl$ and $4pn'l'$, which amounts to 206 configurations. These configurations are used in the configuration-interaction expansion to obtain Zn atom wave functions. We modify the electron-electron interaction by adding a two-electron polarization potential with $\alpha_c=2.6$ and cutoff radius $r_c=2.18$ in order to further model core polarization effects. The cutoff radius r_c of one-

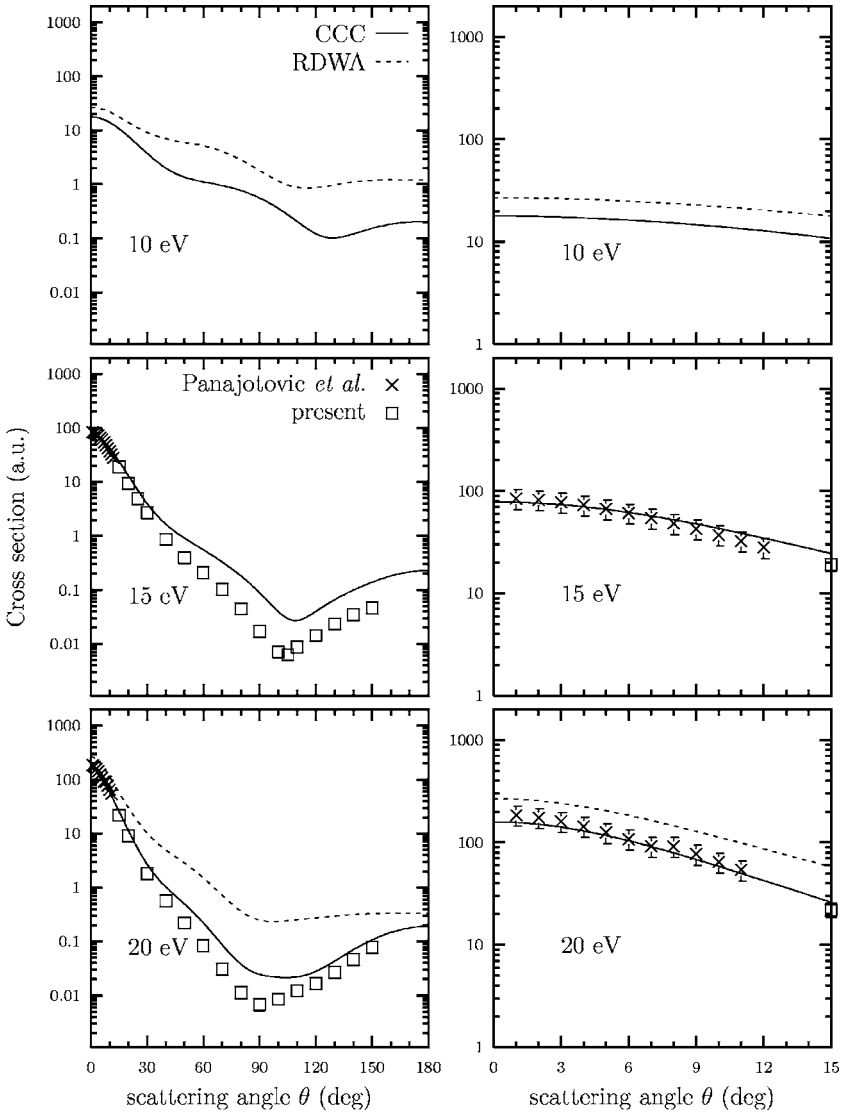

FIG. 1. Differential cross sections for electron impact excitation of the $4s4p\,^1P^o$ state from the ground state of zinc at 10, 15, and 20 eV. The CCC calculations and present experiment are as described in text. The RDWA calculations are due to Kaur *et al.* [6]. Experiment is due to Panajotović *et al.* [5].

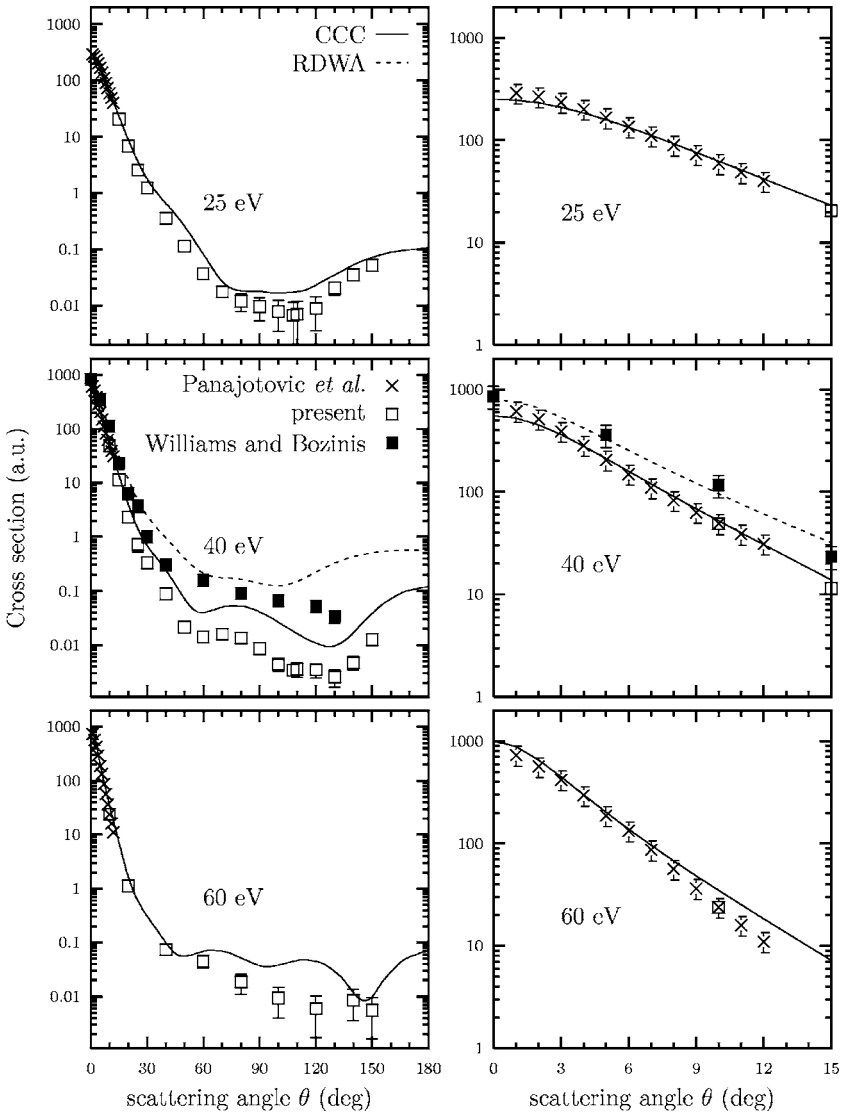

FIG. 2. As for Fig. 1 except for 25, 40, and 60 eV incident energies. Additional experiment is due to Williams and Bozinis [4].

and two-electron polarization potentials has been varied independently to obtain the best fit of the Zn ionization potential and optical oscillator strength for the resonant $4s4p\ ^1P^o - 4s^2\ ^1S$ transition.

In Table I we present ionization energies of negative-energy states, relative to the ground state of the Zn^+ ion for the present CCC calculations. We find very good agreement with experimental data for singlet and triplet S, P, and D symmetries up to the $n=6$ shell and for F symmetry up to the $n=5$ shell. These negative-energy states represent an accurate approximation to the corresponding bound states of the Zn atom. The rest of the negative-energy states together with positive-energy states are the so-called pseudostates and represent a square-integrable representation of the remaining Zn bound states and the continuum, respectively. The maximum energy of the positive-energy states obtained in our calculations is about 14 eV. This, from our experience, is sufficient to model scattering flux to the most important ionization channels.

It is vital, particularly in the context of the present study, to ensure that the optical oscillator strengths (OOS's) are calculated accurately within the Zn structure model. The experimental value for the $4s4p\ ^1P^o$-$4s^4\ ^1S$ transition is 1.47 [16] and for the $4s5p\ ^1P^o$-$4s^4\ ^1S$ transition it is 0.122 [17]. These agree well with our results of 1.47 and 0.11, respectively. These were calculated in the length form using the modified form of the dipole operator [9].

The scattering calculations have been performed using the momentum-space formulation of the close-coupling method as described elsewhere [9,18]. The important modification implemented in the present study deals with the issue of numerical stability of the solution of the Lippmann-Schwinger equations for the T matrix. It is well known that these equations lead to a nonunique half-on-shell T matrix [19,20] although the on-shell T matrix is unique. This property of the Lippmann-Schwinger equation can often lead to a loss of accuracy for calculated on-shell T-matrix elements. The best way to resolve such problems is to modify the kernel of the T-matrix equations in order to project out the nonunique solutions. This approach was implemented for scattering from quasi-one-electron atoms by Bray [21]. In the case of quasi-two-electron atoms Fursa and Bray [18] have used a similar technique for the special case of the frozen-core model of helium. We have generalized this technique to

the case of an arbitrary number of core electrons. In the present case two cores ($4s$ and $4p$) were used. This technique requires the generation of all possible configurations for a given set of one-electron orbitals and specified core orbitals. It is also required that all target states obtained from the diagonalization of the target atom Hamiltonian be included in the scattering calculations which is the reason why such a large number of target states (206) are included in the present close-coupling calculations.

IV. RESULTS

Our new measurements have been performed at 15, 20, 25, 40, and 60 eV for the $4s4p\ ^1P^o$ excitation and at 20, 25, and 40 eV for the $4s5p\ ^1P^o$ excitation. Present experimental DCS's for both transitions are normalized to the earlier measurements [5] at 10° since the measurements [5] were done in the range from 1 (2 for the $5\ ^1P$) to 12°. Thus determined absolute DCS's are presented in Table II for the $4s4p\ ^1P^o$ excitation and Table III for the $4s5p\ ^1P^o$ excitation. We also present in Table IV an estimate of the integrated cross sections for both transitions obtained by integrating over an appropriately extrapolated and interpolated combined DCS data set from the present and earlier low-angle measurements. For extrapolation from 150° to 180°, we have used the CCC-calculated DCS profiles since good agreement in shape exists between theory and experiment.

The DCS's for the $4s4p^1P^o$ excitation from the ground state of zinc are presented in Figs. 1 and 2, and 3 for incident electron energies from 10 eV to 100 eV. The right panels of the figures give the low-angle behavior of the cross sections. Our new measurements are compared with the earlier low-angle data of Panajotović *et al.* [5] and the measurments of Williams and Bozinis [4] at 40 eV. The experimental results are compared with the present CCC calculations and the results of the RDWA calculations [6]. The DCS values of Williams and Bozinis [4] are systematically higher than our measurements at all scattering angles. At small scattering angles the difference is about a factor of 2 and it increases to nearly a factor of 10 at large scattering angles. The CCC calculations agree well with the low-angle measurements of Panajotović *et al.* [5] across all incident electron energies. At larger scattering angles the agreement between the present measurements and CCC calculations is not perfect. In particular, at 40 eV there is nearly factor of 3 discrepancy at about 90°. The RDWA-calculated values are systematically higher than both the experimental and CCC data. At small scattering angles the RDWA calculations are about a factor of 2 higher, which is likely related to less accurate Zn wave functions (larger OOS value of 1.8) in RDWA calculations. However, the large discrepancies both in the DCS shape and absolute values (factor of 10) at larger scattering angles suggest that channel coupling effects are playing a major role. This is not surprising as the $4s4p^1P^o$ DCS is strongly forward peaked and drops by five orders of magnitude as the scattering angles increase and therefore is particularly sensitive to the details of the theoretical model in the region of small cross sections.

In Fig. 4 we present the DCS's for excitation of the $4s5p^1P^o$ state at 20, 25, and 40 eV incident electron energies. We compare the new measurements and CCC results with low-angle measurements of Panajotović *et al.* [5] and, at 40 eV, with the data of Williams and Bozinis [4]. As the value for the $4s5p^1P^o$-$4s^2\ ^1S$ transition OOS in the CCC calculations (0.11) is somewhat smaller than the experimental value of 0.122 [17] we expect that the low-angle CCC DCS's would somewhat underestimate the experimental low-angle

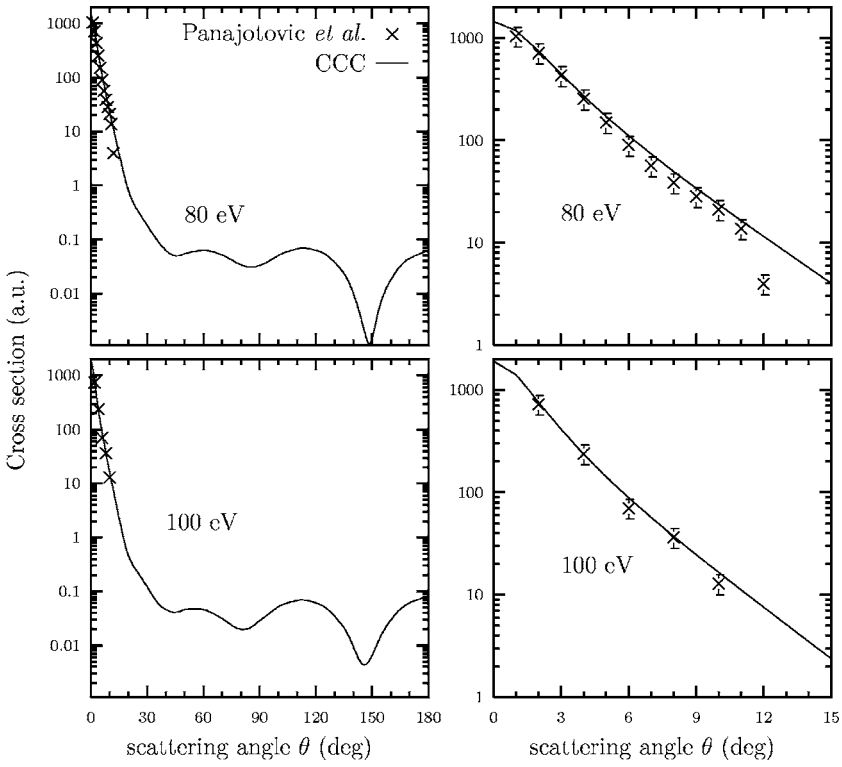

FIG. 3. As for Fig. 1 except for 80 and 100 eV incident energies.

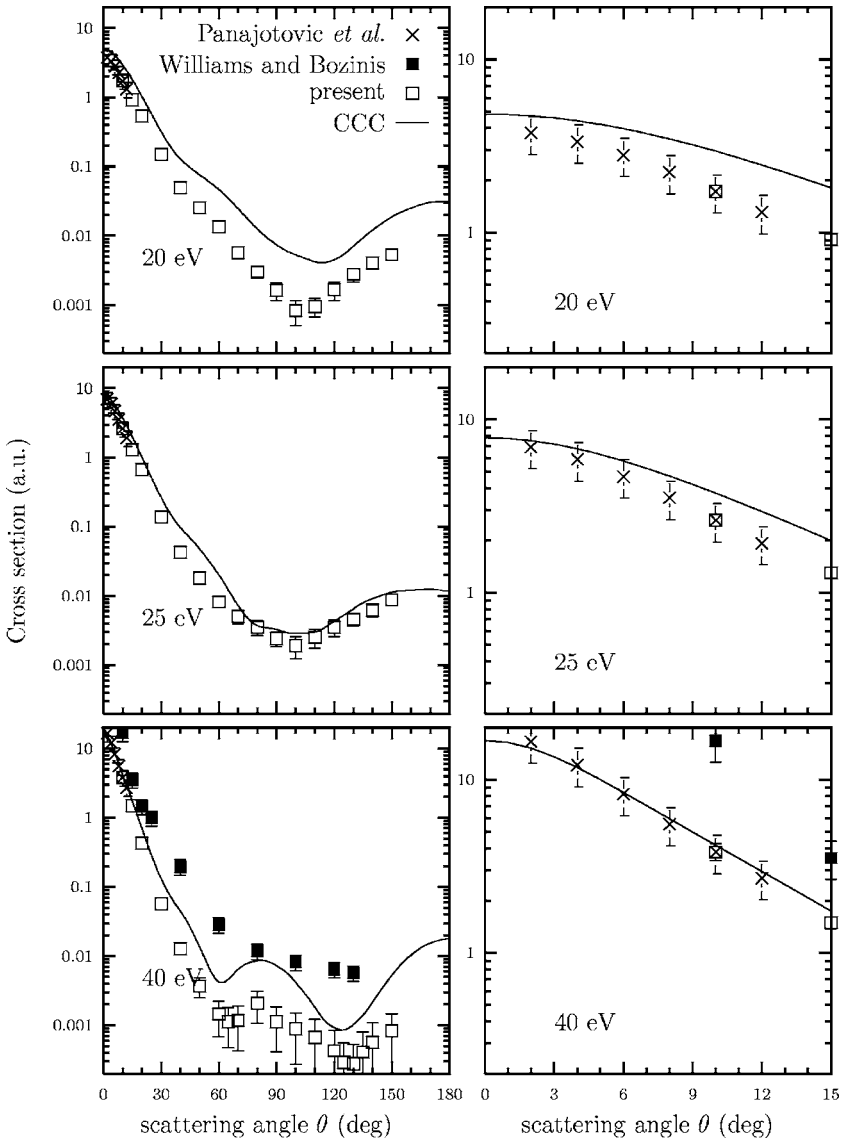

FIG. 4. Differential cross sections for electron impact excitation of the $4s5p\,^1P^o$ state from the ground state of zinc at 20, 25, and 40 eV. Theory and experiment are as for Fig. 2.

DCS's [5]. However, we find that the CCC results are larger than the experimental DCS's at 20 eV, with agreement improving as the incident electron energy increases to 25 eV, with perfect agreement achieved at 40 eV. This is most likely related to the difficulty in normalization of the experimental DCS's [5]. The DCS values measured by Williams and Bozinis [4] at 40 eV are significantly higher than our values over the entire range of scattering angles.

We present the integrated cross sections (ICS's) for excitation of the $4s4p\,^1P^o$ state in Fig. 5. The present experimental and CCC ICS results are compared with the experimental data of Shpenik *et al.* [2], the 40 eV value of Williams and Bozinis [4], and *B*-spline *R*-matrix calculations (BSRM) of Zatsarinny and Bartschat [7]. We find very good agreement between the CCC and BSRM results for incident electron energies below the ionization threshold (9.4 eV) while there are some minor discrepancies at larger energies. The agreement between both calculations and the experimental data of Shpenik *et al.* [2] is excellent at energies below 7.5 eV. At around 7.5 eV the experimental data show a stronger drop in the ICS's than do the CCC and BSRM calculations. This leads to a substantial disagreement between the theoretical and experimental ICS's as the incident energy increases. However, the present experimental ICS's are in good agreement with the data of Shpenik *et al.* [2] at 15 eV, while at higher energies the agreement with the theoretically predicted ICS's is within experimental error. The apparent disagreement between the present 15 eV CCC and experimental ICS's is somewhat unexpected given the good agreement between the CCC and low-angle data of Panajotović *et al.* [5]. The reason for the disagreement is the large contribution from intermediate scattering angles where agreement is not perfect. The 40 eV value of Williams and Bozinis [4] is too high as expected from the DCS results.

In the context of disagreement between the theoretical calculations (CCC and BSRM) and experiment of Shpenik *et al.* [2] it is worthwhile to make a few comments on the the similarities and differences in the CCC and BSRM calculations. The BSRM calculations make use of zinc wave functions which are very similar to those used in the present CCC calculations for low-energy target states. However, a significant difference exists in the description of high-lying

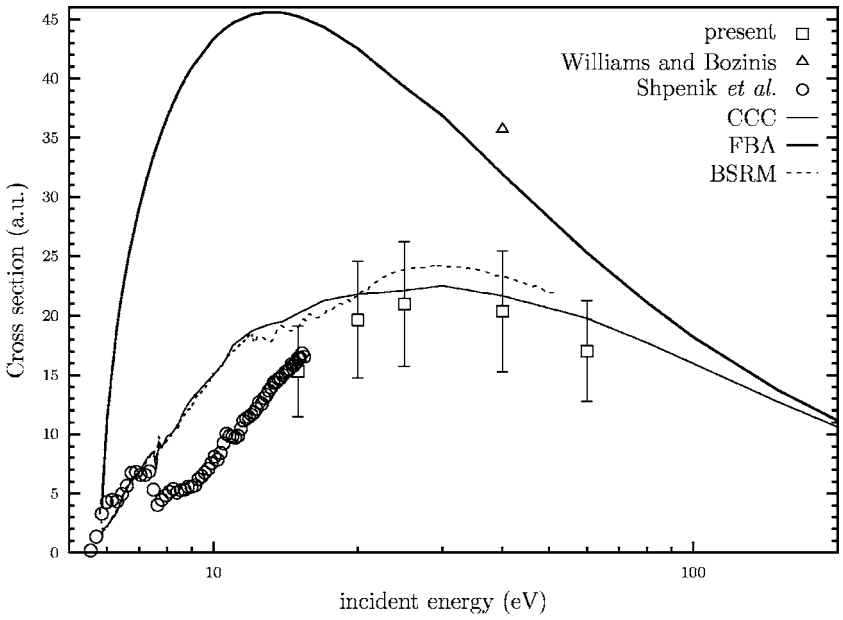

FIG. 5. Integral cross sections for electron impact excitation of the $4s4p\,^1P^o$ state from the ground state of zinc. The CCC and FBA calculations and present experiment are described in text. The *R*-matrix results (BSRM) are due to Zatsarinny and Bartschat [7]. Experiments are due to Shpenik *et al.* [2] and Williams and Bozinis [4].

negative-energy states and pseudostate representation of the target continuum (see Table I in this paper and Table 1 of Zatsarinny and Bartschat [7]) with the present structure model having a larger number of states in the continuum. Another important difference between CCC and BSRM calculations is that the BSRM calculations directly include excitations out of the $4d^{10}$ core in the target structure and scattering calculations while the present CCC calculations make use of phenomenological polarization potentials to model core polarization effects. The CCC and BSRM calculations, therefore, differ substantially in both the zinc structure model and method of scattering calculation. The very good agreement between these two calculations, in particular below the ionization threshold, is very encouraging and lends credit to the reliability of the theoretical results.

Finally, in Fig. 6 we present the ICS's for excitation of the $4s5p\,^1P^o$ state. As for the $4s4p\,^1P^o$ state, we find good agreement between the CCC and BSRM results of Zatsarinny and Bartschat [7] for incident electron energies below the ionization threshold, while there is some disagreement at the higher incident electron energies. The resonance structures which are apparent in the BSRM calculations could be related to excitations out of the $4d^{10}$ core. The present experimental ICS's at 20 and 25 eV disagree with the theoretical results but are in good agreement at 40 eV, as expected from the earlier $4s5p\,^1P^o$ DCS comparison. The 40 eV values of Williams and Bozinis [4] are about 3 times larger.

In Figs. 5 and 6 we also present ICS results from the first Born approximation (FBA) as obtained in the present Zn structure model. We find unusually large differences between the FBA and close-coupling results starting from near threshold (5.8 eV) up to 80 eV. This is an indication of the nonperturbative nature of the excitation process for these transitions and has a number of implications. The validity region

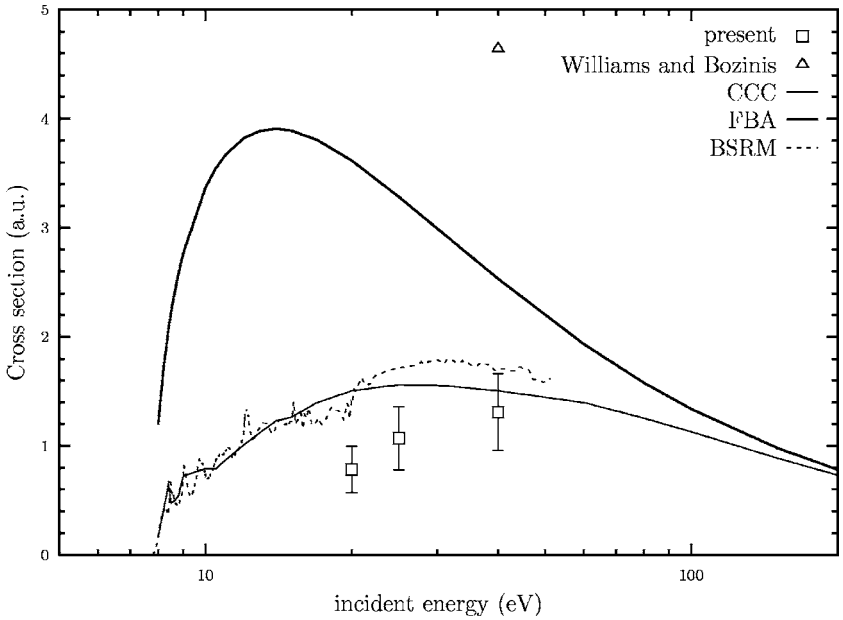

FIG. 6. Integral cross sections for electron impact excitation of the $4s5p\,^1P^o$ state from the ground state of zinc. Experiment and theory are as for Fig. 5.

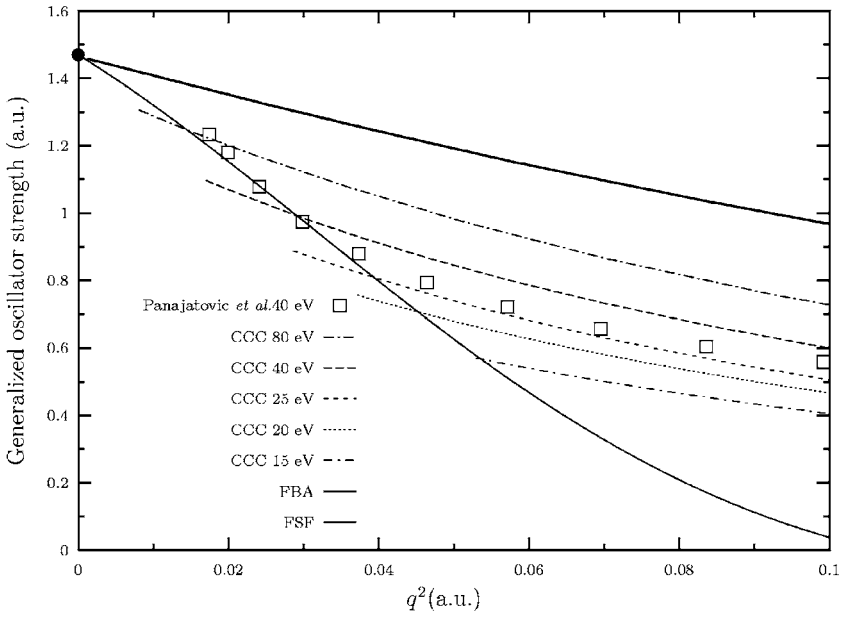

FIG. 7. Generalized oscillator strength for electron impact excitation of the $4s4p\,^1P^o$ state of zinc. The FSF of Felfli and Msezane [23] is compared with present CCC and FBA results and 40-eV low-angle data of Panajotović *et al.* [5].

of the first-order theoretical methods (RDWA, for example) is at higher than usual incident electron energies, as confirmed by the rather poor DCS agreement between the RDWA and CCC results at 40 eV in both shape and absolute values. It also affects the validity of a commonly used normalization procedure for experimental relative DCS's using extrapolation of the generalized oscillator strength (GOS) to the optical limit [22]. In Fig. 7 we have presented GOS for the $4s4p\,^1P^o$-$4s^2\,^1S$ transition obtained in the CCC calculations at 80, 40, 25, and 15 eV together with the GOS obtained using the FBA. We can see that the CCC results for all energies lie well below the FBA result. Linear extrapolation of any of the CCC-calculated GOS curves to zero momentum transfer ($q=0$) does not lead to the optical oscillator strength value (1.47, indicated by the solid circle in Fig. 7). Williams and Bozinis [4] have used this method to put onto the absolute scale their relative DCS measurements for the $4s4p\,^1P^o$ and $4s5p\,^1P^o$ transitions, which we suspect leads to a large normalization error. Felfli and Msezane [23] have suggested to use the forward-scattering function (FSF), presented in Fig. 7, to normalize the relative experimental DCS's. Such normalization was applied to the low-angle measurements of Panajotović *et al.* [5] (40 eV data are presented in Fig. 7) and clearly this is a significant improvement over extrapolation to zero momentum transfer. For the FSF-based normalization procedure to be reliable, the FSF curve should pass though the CCC-calculated GOS at minimum momentum transfer for each incident electron energy. However, examination of Fig. 7 shows that this occurs only at 15 eV, while at larger incident electron energies there is a systematic disagreement of the order of 10%.

V. CONCLUSIONS

We have performed measurements of the DCS for excitation of the $4s4p\,^1P^o$ and $4s5p\,^1P^o$ states form the ground state of zinc for angular region from 10° to 150°. These data complement the earlier low-angle DCS measurements of Panajotović *et al.* [5]. We have also performed CCC calculations for *e*-Zn scattering and presented DCS's and ICS's for the $4s4p\,^1P^o$ and $4s5p\,^1P^o$ excitations. Good agreement has been found between CCC results and low-angle DCS measurements for both transitions. The agreement between the present $4s4p\,^1P^o$ DCS measurements and the CCC results is not perfect, and more work is required to identify the source of the disagreement. We have also found that there is good agreement between the CCC calculations and the recent BSRM results [7] for the $4s4p\,^1P^o$ and $4s5p\,^1P^o$ excitation ICS's. However, theoretical results are in apparent disagreement with recent measurement of the $4s4p\,^1P^o$ excitation function by Shpenik *et al.* [2]. In the future we are planning to extend this work to measurements and calculations of elastic scattering and excitation of a number of low-lying levels of zinc.

ACKNOWLEDGMENTS

The authors would like to thank Professor O. B. Shpenik, Professor K. Bartschat, and Professor R. Srivastava for sending their data in electronic form. This work was supported by the Australian Research Council, the Maui High Performance Computer Center, and Grant No. OI 1424 of the Republic of Serbia.

[1] M. Born, J. Phys. D **34**, 909 (2001).
[2] O. B. Shpenik, I. V. Chernyshova, and E. E. Kontros, Radiat. Phys. Chem. **68**, 277 (2001).
[3] O. B. Shpenik, I. P. Zapesochny, V. V. Sovter, E. E. Kontrosh, and A. N. Zavilopulo, Sov. Phys. JETP **65**, 1797 (1973).
[4] W. Williams and D. Bozinis, Phys. Rev. A **12**, 57 (1975).
[5] R. Panajotović, D. Šević, V. Pejčev, D. M. Filipović, and B. P. Marinković, Int. J. Mass. Spectrom. **233**, 253 (2004).
[6] S. Kaur, R. Srivastava, R. P. McEachran, and A. D. Stauffer, J. Phys. B **30**, 1027 (1997).
[7] O. Zatsarinny and K. Bartschat, Phys. Rev. A **71**, 022716 (2005).
[8] A. Chutjian, J. Chem. Phys. **61**, 4279 (1974).
[9] D. V. Fursa and I. Bray, J. Phys. B **30**, 5895 (1997).
[10] K. Bartschat, O. Zatsarinny, I. Bray, D. V. Fursa, and A. T. Stelbovics, J. Phys. B **37**, 2617 (2004).
[11] D. V. Fursa, I. Bray, and G. Lister, J. Phys. B **36**, 4255 (2003).
[12] D. V. Fursa and I. Bray, in *Correlations, Polarization, and Ionization in Atomic Systems*, edited by D. H. Madison and M. Schulz, AIP Conf. Proc. No. 604 (AIP, Melville, NY, 2002), pp. 145–150.
[13] D. V. Fursa and I. Bray, Phys. Rev. A **63**, 032708 (2001).
[14] D. V. Fursa and I. Bray, Phys. Rev. A **59**, 282 (1999).
[15] S. H. Patil, At. Data Nucl. Data Tables **71**, 41 (1999).
[16] P. S. Doidge, Spectrochim. Acta, Part B **50**, 209 (1995).
[17] D. A. Verner, P. D. Bartel, and D. Tytler, Astron. Astrophys., Suppl. Ser. **108**, 287 (1994).
[18] D. V. Fursa and I. Bray, Phys. Rev. A **52**, 1279 (1995).
[19] D. W. Norcross, J. Phys. B **2**, 1300 (1969).
[20] A. T. Stelbovics and B. H. Bransden, J. Phys. B **22**, L451 (1989).
[21] I. Bray, Phys. Rev. A **49**, 1066 (1994).
[22] E. N. Lassettre, A. Skerbelle, and M. A. Dilon, J. Chem. Phys. **50**, 1829 (1969).
[23] Z. Felfli and A. Z. Msezane, J. Phys. B **31**, L165 (1998).
[24] C. E. Moore, *Atomic Energy Levels*, Natl. Bur. Stand. (U.S.) Circ. No. 467 (GPO, Washington, D.C., 1949), Vol. III.